for each atom calculated from the observed values of b_{ij} and in addition the calculated U_{ij} assuming rigid-body movements.

The agreement of these calculated U_{ij} with the observed values is quite good in most cases, but more detailed tests tend to show that the rings cannot be regarded as true rigid bodies. These calculations have been carried out on the University of St Andrews IBM 1620 machine with a program written by Dr D.M. Burns and Mr J.T.McMullan and we are most grateful for their help.

References

BERGHUIS, J., HAANAPPEL, IJ. M., POTTERS, M., LOOPSTRA, B. O., MACGILLAVRY, C. H. & VEENENDAAL, A. L. (1955). Acta Cryst. **8**, 478.
BULLEN, G. J. (1959). Acta Cryst. **12**, 703.
BULLEN, G. J. (1961). Nature, Lond. **189**, 291.
FREEMAN, A. J. & WOOD, J. H. (1959). Acta Cryst. **12**, 271.
JAMES, R. W. (1948). The Optical Principles of the Diffraction of X-rays, p. 342. London: Bell.
MCWEENY, R. (1951). Acta Cryst. **4**, 513.
ROOF, R. B. (1956). Acta Cryst. **9**, 781.
SCHOMAKER, V., WASER, J., MARSH, R. E. & BERGMAN, G. (1959). Acta Cryst. **12**, 600.

X-ray Measurements of Stacking Faults in Silver-Antimony Alloys

BY S. P. SEN GUPTA,

Department of General Physics & X-rays, Indian Association for the Cultivation of Science, Calcutta-32, India

The Geiger counter X-ray diffractometer has been utilized to record the line profiles from cold-worked silver-base alloys containing pentavalent solute antimony in the primary solid solution range. The deformation-fault probability α and the twin-fault probability β have been obtained from peak shift and peak asymmetry measurements. Peak shifts of the neighbouring pairs 111–200, 200–220 and 220–311 have been considered in the determination of α and a linear dependence of deformation fault probability with increasing solute concentration has been observed. Using Fourier analysis of line profiles, the effective particle sizes $[D_e]_{hkl}$ and root mean square strains $[\langle \varepsilon_l^2 \rangle]_{hkl}^{1/2}$ have been obtained and it has been found that both are anisotropic in nature and vary considerably with increasing solute content. The role of stacking faults in the particle size broadening has been found to be significant and a fair agreement exists in the values of the compound fault probability $(1 \cdot 5\alpha + \beta)$ evaluated by two different methods.

Introduction

During recent years considerable attention has been given to the presence and effects of stacking faults in f.c.c. metals and alloys. Extensive studies have been made in binary alloys based on the solvent metals copper, silver and gold (Warren & Warekois, 1955; Wagner, 1957; Smallman & Westmacott, 1957; Vassamillet, 1961; Davies & Cahn, 1962; Adler & Wagner, 1962; Foley, Cahn & Raynor, 1963; Vassamillet & Massalski, 1964; Wagner & Helion, 1965; Sen Gupta & Quader, 1966; Goswami, Sen Gupta & Quader, 1966) and from these investigations it has been observed that (i) the stacking fault probability α increases rapidly with increasing solute content, (ii) the increase is either linear or roughly parabolic and (iii) the variation of α with composition is primarily determined by the electron/atom ratio, but that for a fixed electron-atom ratio, α increases as the solute valency increases. But these investigations, in general, are concerned with solid solutions of di,- tri-, or tetra-valent solutes in solvent metals copper, silver and gold and measure-ments with pentavalent solute were lacking. Very recently, Sastry, Rama Rao & Anantharaman (1965) have determined the stacking-fault densities in alloys of silver with pentavalent solute element antimony and observed that the variation of α with electron-atom ratio is similar to the trends observed by Davies & Cahn (1962) for silver- and copper-base alloys.

The present investigation deals with silver-antimony alloys in the primary solid solution range and seeks to give a fairly detailed picture of the deformed state in this system from peak position, peak asymmetry and peak broadening measurements using the conventional methods. This will also form an extension of the previous measurements with di-, tri- and tetra-valent solutes in silver, *i.e.* in solvent of the same period as the solutes.

Experimental results

Sample preparation and experimental procedure

The preparation of alloys from spectrographically standardized silver and antimony supplied by Johnson, Matthey & Co., Ltd, London, follows the same method

as adopted previously (Sen Gupta & Quader, 1966), the homogenization temperature being 700–800 °C.

Cold-working was carried out by hand filing at room temperature (28 ± 1 °C). A sample of the filings was retained in the 'as-filed' condition and another sample was annealed at 600 °C for 4 hours in a Pyrex glass capsule sealed under vacuum. The line profiles of the 111, 200, 220, 311, 222 and 400 reflexions were recorded at room temperature (28 ± 1 °C) with a standard Philips Geiger counter X-ray diffractometer (PW 1050, 1051) using nickel filtered Cu $K\alpha$ radiation from a highly stabilized X-ray generator (PW 1010) in the same manner as described earlier (Sen Gupta & Quader, 1966).

Estimation of stacking faults

The deformation fault probability α was obtained from the neighbouring pairs of 111–200, 200–220 and 220–311 reflexions using the relation (Wagner, 1957):

$$(2\theta^\circ_{hkl} - 2\theta^\circ_{h'k'l'})_{cw} - (2\theta^\circ_{hkl} - 2\theta^\circ_{h'k'l'})_{Ann} = H \cdot \alpha \quad (1)$$

and

$$H = (\langle G \rangle j \cdot \tan \theta^\circ)_{hkl} - (\langle G \rangle j \cdot \tan \theta^\circ)_{h'k'l'} \quad (2)$$

where j is the fraction of (hkl) planes affected by deformation faults, $G = (\pm)90\sqrt{3} \cdot h_3/\pi^2 l^2_o$ and $\langle G \rangle$ is the averaged value for the hkl reflexions affected by deformation faults.

The peak positions of 111, 200, 220 and 311 reflexions were determined by taking the mid-points of section lines drawn parallel to the background level and extrapolating to the peak maximum. The estimated accuracy in 2θ of the determination of the peak maximum position is about $\pm 0.01°$ for 2θ less than 70° and $\pm 0.02°$ for 2θ of larger values. Table 1 summarizes the values of α together with the values of $(2\theta^\circ_{hkl} - 2\theta^\circ_{h'k'l'})_{cw} - (2\theta^\circ_{hkl} - 2\theta^\circ_{h'k'l'})_{Ann}$ measured from the separations of the 200–111, 220–200 and 311–220 peaks for the silver–antimony filings with increasing antimony content. By comparing the signs of the peak separation (Table 1) it can be seen that the theory (Paterson, 1952) predicts the shifts in the right directions. The values of α computed from the change in separations of the 200–111 and 220–200 peaks agree well for the four alloy compositions, whereas this was not satisfied for those obtained from the change in separation of the 311–220 peaks at higher solute content. This may be due to the error involved in peak maximum position determination as the 311 peak becomes very much broad at higher solute content.

Twin faults have been found to broaden the diffraction line profiles asymmetrically. The asymmetry may also be produced by the segregation of the solutes to the stacking faults, according to the theory of Willis (1959). But this effect will be very small in the present case owing to similar scattering power of the solute and the solvent atoms. A similar procedure (Sen Gupta & Quader, 1966) has been adopted in the determination of β from cold-worked 111 and 200 peaks using the relation (Cohen & Wagner, 1962):

$$\beta = \frac{\Delta C.G.(°2\theta)_{111} - \Delta C.G.(°2\theta)_{200}}{11 \tan \theta_{111} + 14 \cdot 6 \tan \theta_{200}} \quad (3)$$

Values of β and the average values of α for Ag–Sb alloys are inserted in Table 2. Figs. 1 and 2 show the variation of α with solute content and electron/atom ratio respectively for Ag–Sb alloys together with Ag–Cd, Ag–In and Ag–Sn alloys (Adler & Wagner, 1962; Sen Gupta & Quader, 1966).

Line shape analysis

Warren and Averbach's method (Warren, 1959) of Fourier analysis of line shapes provides information concerning the effective particle size D_e, the root mean square strain components $\langle \varepsilon^2_L \rangle^{\frac{1}{2}}$ and the compound fault density $(1 \cdot 5\alpha + \beta)$. The 111, 222, 200 and 400 reflexions were chosen as with these it is possible to determine particle sizes and lattice strains in [111] and [100] directions. Stokes's (1948) corrected Fourier coefficients expressing the line shapes were obtained by means of Beevers–Lipson strips and the effective particle size D_e and the r.m.s. strain components $\langle \varepsilon^2_L \rangle^{\frac{1}{2}}$ were then evaluated by using the Warren–Averbach technique (Warren, 1959). In applying Stokes's (1948) method it has been assumed that line shapes obtained from the samples annealed for 4 hours at 600 °C are, in each case, an exact measure of instrumental broadening. The effective particle size D_e may be written in

Table 1. *Peak shifts and deformation stacking fault probabilities* (α) *in cold-worked silver–antimony alloys*

Composition (at. %)	hkl	$h'k'l'$	Peak shift (°)	$\alpha \times 10^3$	$\langle \alpha \rangle \times 10^3$
Ag–1·33 Sb	200	111	−0·045	9·84	
	220	200	+0·060	10·53	11·37
	311	220	−0·050	13·74	
Ag–2·66 Sb	200	111	−0·095	20·79	
	220	200	+0·115	20·22	21·48
	311	220	−0·085	23·42	
Ag–4·00 Sb	200	111	−0·150	32·96	
	220	200	+0·180	31·77	29·41
	311	220	−0·085	23·51	
Ag–5·35 Sb	200	111	−0·175	38·59	
	220	200	+0·215	38·08	36·20
	311	220	−0·115	31·93	

terms of the coherent domain size D normal to the reflecting planes, the deformation and twin fault probability α and β, the domain size T in the faulting plane and the lattice parameter a (Warren, 1961):

$$\frac{1}{[D_e]_{111}} = \frac{1}{D} + \frac{1}{\sqrt{2}T} + \frac{\sqrt{3}}{4a}(1\cdot5\alpha+\beta) \qquad (4)$$

$$\frac{1}{[D_e]_{100}} = \frac{1}{D} + \frac{1}{\sqrt{1\cdot5}T} + \frac{1}{a}(1\cdot5\alpha+\beta). \qquad (5)$$

The inverse of the last term is referred to as D_{SF}, the fictitious domain size due to faulting. A minimum value of T, T_{min} is given by (Warren, 1961):

$$T_{min} = \frac{0\cdot82}{\left[\dfrac{2\cdot31}{[D_e]_{111}} - \dfrac{1}{[D_e]_{100}}\right]}. \qquad (6)$$

By measuring D_e in two crystallographic directions [111] and [100] it is also possible to evaluate the compound fault density $(1\cdot5\alpha+\beta)$ from the relation (Wagner & Aqua, 1963):

$$(1\cdot5\alpha+\beta)_B = 1\cdot76a \cdot x[(D_e)_{111}$$
$$-(D_e)_{100}]/[(D_e)_{111} \cdot (D_e)_{100}] \qquad (7)$$

where $x=1$ for the Warren–Averbach method.

Table 2 summarizes the values of $[D_e]_{hkl}$, D_{SF}, T_{min}, $(1\cdot5\alpha+\beta)$ and $[\langle\varepsilon^2_{L=50A}\rangle]^{1/2}_{hkl}$ (r.m.s. strain at an averaging distance of $L=50$ Å) for Ag–Sb alloys. Fig.3 illustrates the decrease in effective particle size and reciprocal stacking fault probability as the solute content is increased in the alloys and Fig.4 shows the variation of $\langle\varepsilon^2_L\rangle^{\frac{1}{2}}$ as a function of distance L for both [111] and [100] directions in the Ag-5·35 Sb alloy.

Discussion

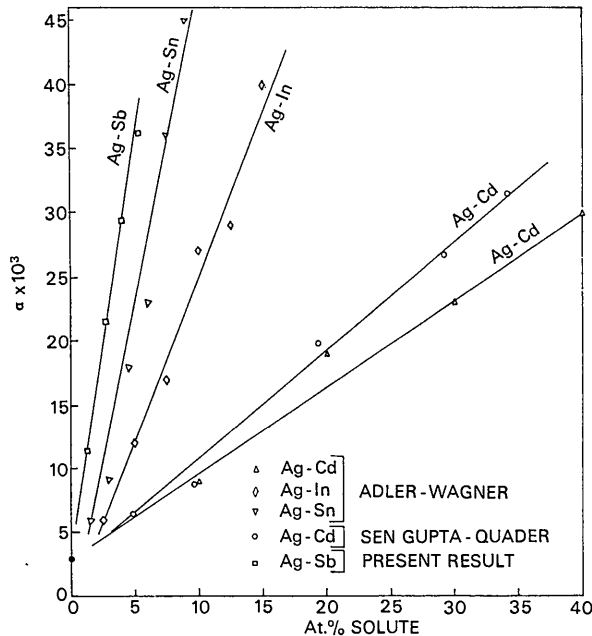Adler & Wagner (1962) in their studies with Ag–Cd, Ag–In and Ag–Sn alloys in the primary solid solution

Fig.1. Deformation fault probability α as a function of solute concentration in silver-base alloys.
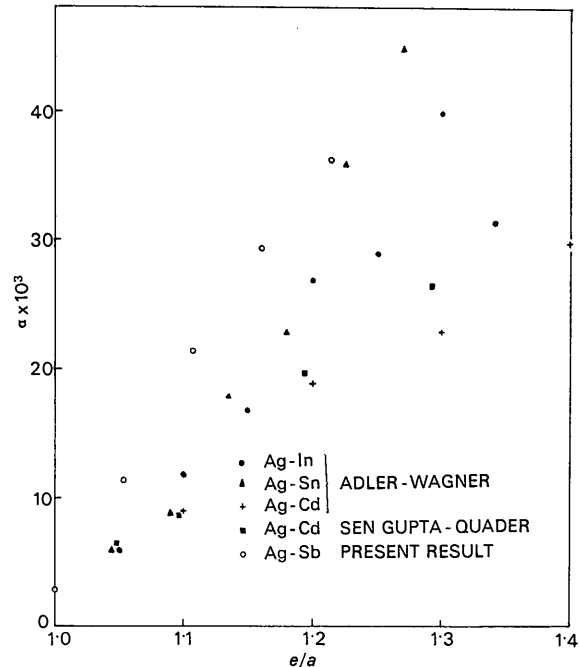

Fig.2. Deformation fault probability α as a function of electron concentration in silver-base alloys.

Table 2. *Experimental results for silver–antimony alloys*

Composition (at. %)	$\langle\alpha\rangle \times 10^3$	$\beta \times 10^3$	$(1\cdot5\alpha+\beta)_{M+A}$ $\times 10^3$	$(1\cdot5\alpha+\beta)_B$ $\times 10^3$	$[D_{SF}]_{111}$ (Å)
Ag–1·33 Sb	11·37	14·70	32	53	298
Ag–2·66 Sb	21·48	26·14	58	63	162
Ag–4·00 Sb	29·41	28·72	73	77	130
Ag–5·35 Sb	36·20	41·47	96	82	99

Composition (at. %)	$[D_e]_{111}$ (Å)	$[D_e]_{100}$ (Å)	$\dfrac{[D_e]_{111}}{[D_e]_{100}}$	T_{min} (Å)	$[\langle\varepsilon^2_{L=50A}\rangle]^{\frac{1}{2}}_{111}$ $\times 10^3$	$[\langle\varepsilon^2_{L=50\,A}\rangle]^{\frac{1}{2}}_{100}$ $\times 10^3$
Ag–1·33 Sb	136	68	2·0	360	2·0	3·7
Ag–2·66 Sb	117	58	2·0	328	2·8	3·8
Ag–4·00 Sb	103	49	2·1	406	3·7	4·1
Ag–5·35 Sb	84	43	1·9	193	4·6	5·4

range have observed a linear dependence of deformation fault probability α with increasing solute content, as also have Sen Gupta & Quader (1966) in Ag–Cd alloys. The present investigation with pentavalent solute antimony in silver-base alloys has also revealed the same nature (Fig. 1), and for a fixed amount of solute present the deformation fault proability is higher in this system as compared with others. It appears from Fig. 2 that the fault probability α, when plotted
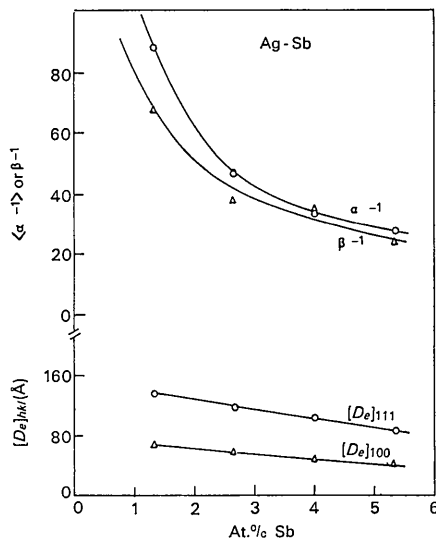

Fig. 3. Variation of reciprocal deformation fault probability α^{-1}, reciprocal twin fault probability β^{-1}, and the effective particle size in the [hkl] directions $[D_e]_{hkl}$ as a function of antimony concentration in silver-base alloy.
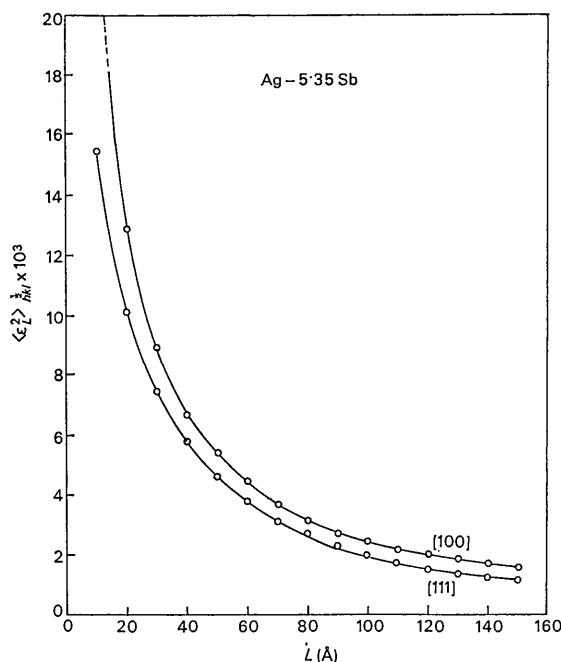

Fig. 4. Variation of r.m.s. strains $\langle \varepsilon_L^2 \rangle^{\frac{1}{2}}$ as a function of distance L for the [111] and [100] directions for cold-worked Ag–5·35 Sb alloy.

as a function of electron/atom ratio, increases with electron concentration, and that for fixed e/a, α increases in the order Ag–Cd, Ag–In, Ag–Sn and Ag–Sb. This is quite consistent with the fact that, for fixed e/a, fault probability increases with the increase of solute valency and this has also been observed by Davies & Cahn (1962) in some copper- and silver-base alloys and by Goswami, Sen Gupta & Quader (1966) in copper-base alloys. Sastry, Rama Rao & Anantharaman (1965) have, of course, reported a higher value of fault probability for the highest concentration of solute antimony in the silver-base alloy (i.e. for approximately Ag–5·35 Sb alloy).

If we assume that there exists a roughly inverse relationship between the stacking fault probability α and the stacking fault energy γ (Vassamillet, 1961), then the form of the curve showing the decrease of α^{-1} with increasing solute content (Fig. 3) is in qualitative agreement with the electron microscope observations of the stacking fault energy variations in silver-base alloys by Art, Gevers & Amelinckx (1964).

Corresponding to the increase in α with solute concentration, the twin fault probability β also increases with increasing solute content (Table 2) and the concentration of twin faults appears to be more. However, systematic variations are not observed and this is due to the fact that the determination of β suffers from experimental limitations (Sen Gupta & Quader, 1966).

The effective particle sizes and lattice strains vary with crystallographic directions and solute content, as is evident from Table 2 and Figs. 3 and 4. As is apparent from Fig. 3, the decrease of effective particle sizes with increasing solute content is linear, and this linearity has also been observed in other silver-base alloys (Adler & Wagner, 1962; Sen Gupta & Quader, 1966). The decrease of effective particle sizes and the reciprocal fault probability with the increase of solute concentration (Fig. 3) implies the significant contribution of stacking faults in the observed particle size broadening. This is clearly borne out by the fact that the average experimental ratio of $[D_e]_{111}/[D_e]_{100}$ is very close to the theoretically predicted value of 2·3 for $[D_e]_{111}/[D_e]_{100}$ and the computed values of $[D_{SF}]$ also agree fairly well with $[D_e]$ obtained from line broadening (Table 2). The influence of D and T (as appears from T_{min} values) seems to be small and the stacking faults tend to extend over rather large distances which are comparable to the coherent domain dimensions D. It has also been observed (Table 2) that the values of $(1·5\alpha + \beta)_B$ obtained from the measured anisotropic particle sizes [equation (7)] are in fair agreement with the values of $(1·5\alpha + \beta)_{M+A}$ obtained from peak maxima and peak asymmetry measurements. This agreement, however, substantiates the experimental measurements.

The r.m.s. strains at an averaging distance of $L = 50$ Å have been found to increase gradually with increasing solute content in both directions (Table 2) and the average ratio of strains measured at $L = 50$ Å is about 1·3, which falls between the ideal cases of iso-

tropic stresses and isotropic strains. This has also been observed for Ag–Cd (Sen Gupta & Quader, 1966) and for Ag–In and Ag–Sn alloys (Adler & Wagner, 1962). Fig. 4 shows the variation of r.m.s. strains as a function of distance L normal to the reflecting planes for the Ag–5·35 Sb alloy, and the same general behaviour was shown by all the specimens and by several f.c.c. alloys of silver and copper. The rapid decrease with increasing L indicates the inhomogeneity of strains and the trend of the curves at higher L is quite consistent with the fact that owing to long range interactions of stresses around a dislocation, the positive and negative stresses balance at some average distance away from the source of stress reaching an asymptotic value.

References

ADLER, R. P. I. & WAGNER, C. N. J. (1962). *J. Appl. Phys.* 33, 3451.

ART, A., GEVERS, R. & AMELINCKX, S. (1964). *Proc. European Regional Conf. Electron Microscopy (Prague)*, p. 223.

COHEN, J. B. & WAGNER, C. N. J. (1962). *J. Appl. Phys.* 33, 2073.

DAVIES, R. G. & CAHN, R. W. (1962). *Acta Metallurg.* 10, 621.

FOLEY, J. H., CAHN, R. W. & RAYNOR, G. V. (1963). *Acta Metallurg.* 11, 355.

GOSWAMI, K. N., SEN GUPTA, S. P. & QUADER, M. A. (1966). *Acta Cryst.* 21, 243.

PATERSON, M. S. (1952). *J. Appl. Phys.* 23, 805.

SASTRY, D. H., RAMA RAO, P. & ANANTHARAMAN, T. R. (1965). *Phys. Status Solidi*, 8, K95.

SEN GUPTA, S. P. & QUADER, M. A. (1966). *Acta Cryst.* 20, 798.

SMALLMAN, R. E. & WESTMACOTT, K. H. (1957). *Phil. Mag.* 2, 669.

STOKES, A. R. (1948). *Proc. Phys. Soc.* B, 61, 382.

VASSAMILLET, L. F. (1961). *J. Appl. Phys.* 32, 778.

VASSAMILLET, L. F. & MASSALSKI, T. B. (1964). *J. Appl. Phys.* 35, 2629.

WAGNER, C. N. J. (1957). *Acta Metallurg.* 5, 427.

WAGNER, C. N. J. & AQUA, E. N. (1963). *Advanc. X-ray Analysis*, 7, 46.

WAGNER, C. N. J. & HELION, J. C. (1965). *J. Appl. Phys.* 36, 2830.

WILLIS, B. T. M. (1959). *Acta Cryst.* 12, 683.

WARREN, B. E. (1959). *Progr. Metal Phys.* 8, 147.

WARREN, B. E. (1961). *J. Appl. Phys.* 32, 2428.

WARREN, B. E. & WAREKOIS, E. P. (1955). *Acta Metallurg.* 3, 473.

The Crystal and Molecular Structure
of Bis(hydrazinecarboxylato-N', O)manganese(II) Dihydrate

BY A. BRAIBANTI, A. TIRIPICCHIO, A. M. MANOTTI LANFREDI AND M. CAMELLINI

Istituto di Chimica generale, Università di Parma, Italy

The crystals of bis(hydrazinecarboxylato-N',O)manganese(II) dihydrate, Mn(II)(N'H₂–NH–COO)₂. 2H₂O, are orthorhombic, space group *Pba*2. The structure, determined from three-dimensional data, consists of chains formed by two types of *trans,cis,cis*-octahedral chelates, bound together in the chain by bridging hydrazinecarboxylato groups. Some water molecules are coordinated to the metal and some are water of crystallization. Four corners of the coordination octahedra of the first type are occupied by hydrazinecarboxylato chelate groups and two by oxygen atoms of bridging hydrazinecarboxylato groups. The complexes of the second type have the same geometrical arrangement of donor atoms as the complexes of the first type except that two water molecules replace the bridging groups. Some of the hydrazinecarboxylato groups behave as tridentate (chelate and bridging) ligands and some as bidentate chelate ligands. The complexes can be compared with octahedral complexes of the same and of different stereochemical arrangements formed by hydrazinecarboxylic acid. The chains of complexes are held together in the crystal by strong hydrogen bonds either direct chain-to-chain or *via* water of crystallization.

Introduction

Determinations of the crystal structures of compounds formed by hydrazinecarboxylic acid, N'H₂–NH–COOH (hycH) with bivalent metals (Ferrari, Braibanti, Bi-

gliardi & Lanfredi, 1965; Braibanti, Manotti Lanfredi & Tiripicchio, 1966; Braibanti, Bigliardi, Manotti Lanfredi & Tiripicchio, 1966; Braibanti, Tiripicchio, Manotti Lanfredi & Bigoli, 1966) have shown that this ligand invariably gives origin to chelates. The com-